Indian Journal of Chemistry
Vol. 61, February 2022, pp. 192-200

Molecular modeling and ADMET predictions of flavonoids as prospective aromatase inhibitors

Karan Gandhi[a], Umang Shah*[a], Samir Patel[a], Mehul Patel[a], Sandip Patel[a], Ashish Patel[a], Swayamprakash Patel[a], Nilay Solanki[a], Ashish Shah[b] & Dharmendra Baria[c]

[a] Ramanbhai Patel College of Pharmacy, Charotar University of Science and Technology, Charusat Campus, Changa 388 421, India

[b] Department of Pharmacy, Sumandeep Vidyapeeth, Piparia, Vadodara 391 760, India

[c] A. R. College of Pharmacy, V. V. Nagar 388 120, India

E-mail: umangshah.ph@gmail.com

Received 21 May 2020; accepted (revised) 26 October 2021

With the advent of a myriad of treatment possibilities for breast cancer, enzyme inhibition turns out to be the prevailing strategy for inhibiting estrogen biosynthesis. Aromatization of ring A of androstenedione, testosterone and 16α-hydroxytestosterone results in increased estrogen level, which embraces the risk for breast cancer. In this present research, we have targeted human placental aromatase complexed with HDDG046 (PDB ID: 4GL7) for its inhibition by several inhibitors of flavonoid derivatives and further screening those molecules for ADMET properties for assessing its credibility for acceptance in successive steps of drug discovery. Novel flavonoid derivative molecules have been designed using Maestro 10.4, based on the literature review. Further, their molecular modeling studies have been performed against the imported target PDB ID: 4GL7 using the GLIDE platform and have been subjected to ADMET assessment using the QikProp and pkCSM program. From all the series exposed to molecular modeling; **2K, 4K, 6K, 8W** and **10K** molecules have been subjected to ADMET study based on their interaction profile. Successively screening of these molecules led to selection of **8W** molecule for further validation by pkCSM. The results obtained have been compared with the reported molecule HDDG046 which presents substantially positive outcomes for **8W** in terms of $CaCo_2$ permeability, water solubility, P- glycoprotein; hERG I, II and CYP interactions, hepatotoxicity, LD50 value and so forth. Juxtaposing the results of all the designed molecules under study, we have established that these prospective molecules especially **8W** of flavonoid derivatives have the potency to inhibit the target under study, which can be useful in the treatment of breast cancer. This has been estimated based on the *in silico* approaches performed using Molecular Modeling which utilizes the integral function of Molecular Mechanics and Quantum Mechanics. In addition, the ADMET predictions validate their integrity for being the lead molecules in drug discovery stages in the near future.

Keywords: Molecular modeling, flavonoids, aromatase inhibitors, breast cancer, ADMET, pkCSM

DNA damage and genetic mutations that are swayed by the hormone estrogen in women is responsible for inducing breast cancer[1]. Early occurrence of menstruation and delayed menopause which is associated with ovarian steroidogenesis is the identifiable risk factors for causing breast cancer. Most importantly, the aromatizations of ovarian and adrenal androgens are the prominent causal factors. This has been experimentally established by provoking mammary adenocarcinomas by higher doses of estrogen. Whilst, the low doses administered over longer duration induced fibro adenomas[2,3]. This aromatization in humans is possible by androstenedione (ASD), testosterone (TST) and 16α-hydroxytestosterone (HTST) with the help of aromatase enzyme which results into formation of C_{18}-estrogens: esterone (E1), 17β–estradiol (E2) and 17β, 16α–estriol (E3) respectively (Figure 1). In this regard, aromatization of A ring occurs due to cascading oxidation of angular C_{19}-methyl group of ASD, TST and HTST[4].

Estrogen biosynthesis can be inhibited by the use of Aromatase inhibitors (AI's) such as exemestene, letrozole and anastrozole. These 3rd generation AI's are used for treating hormone receptor- positive breast cancer in postmenopausal women[7,8]. Tamoxifen, being

Abbreviations: ADMET: Absorption, Distribution, Metabolism, Excretion and Toxicity; PDB: Protein Data Bank; HER: Heregulin; SERM: Selective Estrogen Receptor Modulator; OPLS: Optimized Potentials for Liquid Simulations; RMSD: Root Mean Square Deviation; MET: Methionine; ARG: Arginine; LEU: Leucine; SER: Serine; PHE: Phenylalanine; VAL: Valine; ASH: Aspartate; ALA: Alanine; ASD: Androstenedione; TST: Testosterone; HTST: Hydroxytestosterone; TRP: Tryptophan; ILE: Isoleucine.

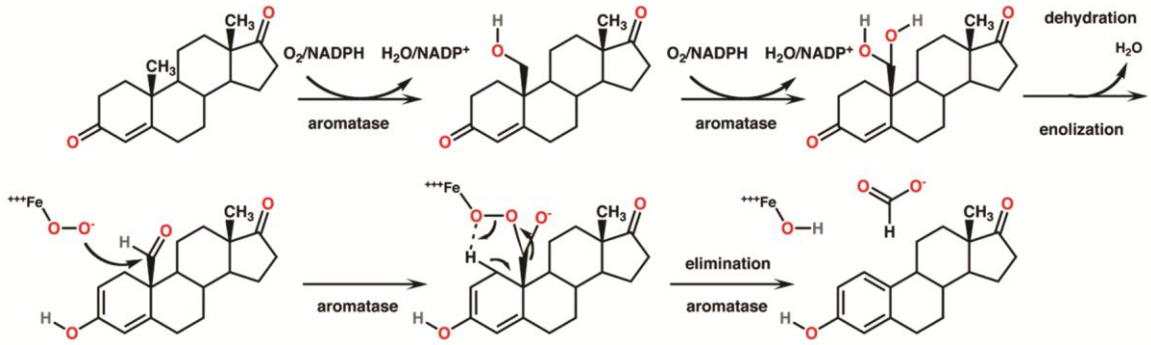

Figure 1 — Mechanism of aromatization by aromatase enzyme

a substantial hormonal anti-cancer drug has both estrogenic and anti-estrogenic biological activities, is used as an adjuvant therapy with AI's and so it is categorized as selective estrogen receptor modulator (SERM). However, it harbors side effects[9-11]. To bolster this claim, a study was conducted among 241 women which revealed that women on a prolonged tamoxifen therapy for more than 12 months reported side effects more frequently than those on a shorter therapy duration. The most common side effects were intense warmness, vaginal dryness, depression and irritation[12].

Natural products like stilbenes, chalcones and flavonoids are also considered as AI's. Most importantly, stilbenes have been reported for its activity for suppressing inflammation, proliferation and also used as an anti-mitotic agent. The anti-inflammatory action of α -viniferin (Figure 2) was established experimentally by administering it more than 3mg/kg intravenously to the mice suffering from paw edema. Additionally, the IC_{50} value was estimated to be 4.9μM and the mechanism involved in it is cyclooxygenase-2 inhibition[13-18]. Flavonoids are C_{15} carbon skeleton with a heterocyclic pyran ring associated with two benzene rings. In addition, they are classified as flavone, flavonols, flavan-3-ols, xanthones, isoflavone, coumarin, flavanonol, flavanone, catechins and anthocyanidins. Moreover, the identifying feature between flavonoids and isoflavanoids is the position of benzenoid group while, between flavonols and flavanones is the presence/absence of –OH group at C-3 and an unsaturated double bond between 2nd and 3rd carbon[19-21].

A literature review was conducted to examine different compounds that were obtained both naturally and synthetically for biological evaluation against aromatase activity in breast cancer. Primarily, anti-aromatase activity was witnessed by the use of

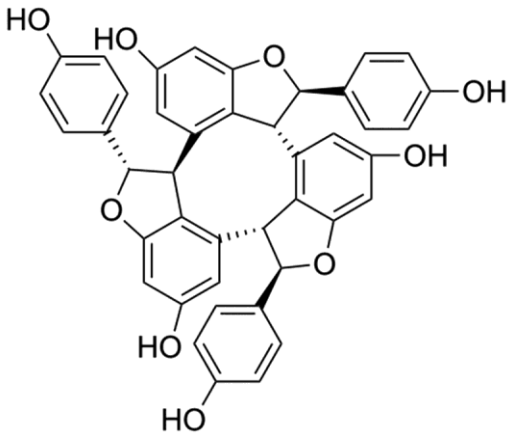

Figure 2 — Structure of α-viniferin

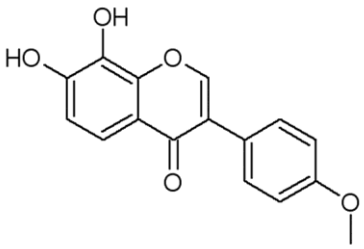

Figure 3 — Structure of Biochanin A

isoflavone, biochanin A (Figure 3) with MCF-7 and SK-BR-3 cancer cell lines. This activity was linked with the subdued mRNA expression[22]. The binding characteristics by flavone and isoflavone have been studied using computer modeling and it was found that these compounds bind to the active site of aromatase in an orientation in which their ring–A and –C mimic ring–D and –C of the steroidal substrate, and many aromatase inhibitors having steroidal ring system. Hence, flavonoid skeleton is selected for the computational study[23,24]. Successively, synthetically derived flavonoids were studied from the literature review for its inhibiting activity for aromatase and depending upon[25-32]. In this present study, we

designed several flavonoids and performed *in-silico* studies to find out novel flavonoids as aromatase inhibitors with ADMET prediction (Figure 4).

The blend of molecular mechanics and quantum mechanics in molecular modeling has been a prodigy for examining vivid parameters of biological systems such as potential active site, hydrophobic/hydrophilic regions, clusters and interactions with the proteins and enzymes. The ligand-protein interaction is essential to be unraveled to design several novel molecules, which binds with the target to modulate or mimic the activity of the proteins. This aim has been successfully accomplished with the help of *in silico* studies which is also known as computer-aided drug designing with the help of software like maestro, gold, glide, autodock, guassian, swissdock, UCSFchimera and many more[33-35].

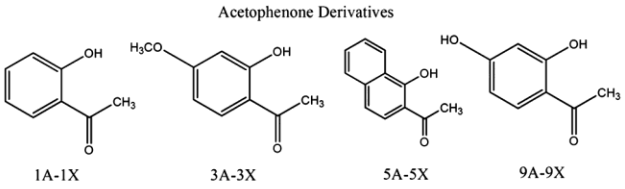

Aldehyde Derivatives

A. Veratraldehyde	M. 2,4,6-Trimethoxybenzaldehyde
B. 3-Hydroxybenzaldehyde	N. 2,3-Dimethoxybenzaldehyde
C. 4-Methoxybenzaldehyde	O. 4-Ethoxy-3-Methoxybenzaldehyde
D. 4-Chlorobenzaldehyde	P. 2,4-Dimethoxybenzaldehyde
E. 4-Fluorobenzaldehyde	Q. 4-Bromobenzaldehyde
F. 3-Chlorobenzaldehyde	R. Benzaldehyde
G. 3-Methoxybenzaldehyde	S. 3-Bromobenzaldehyde
H. Pyrolle 2-Carboxyldehyde	T. 2,4-Dihydroxybenzaldehyde
I. Pyridine 2-Carboxyldehyde	U. 3,4-Dihydroxybenzaldehyde
J. Pyridine 3-Carboxyldehyde	V. 2-Imidazolecarboxyldehyde
K. Pyridine 4-Carboxyldehyde	W. 4-Imidazolecarboxyldehyde
L. Cinnamaldehyde	X. 1-Methyl-2-Imidazolecarboxyldehyde

Figure 4 — Several flavonoid derivatives subjected to *in silico* studies.

Materials and Methods

Retrieving of Target Enzyme

In this present research, we have selected the target enzyme as human placental aromatase complexed with designed inhibitor HDDG046 (PDB ID: 4GL7) (Figure 5). The crystal structure has been obtained from protein data bank[7]. The retrieved aromatase structure consists of 10,13-dimethyl-6-(pent-2-yn-1-yloxy)-7, 8, 9, 10, 11, 12, 13, 14, 15, 16-decahydro-3H-cyclopenta phenanthrene-3,17(6H)-dione, as a ligand bound to it. Ghosh D *et. al.* designed and validated this ligand molecule with target PDB ID: 4GL7 using molecular docking.

Figure 5 — Crystal structure of 4GL7 placental aromatase complexed with HDDG046

Protein Preparation

Protein preparation feature of maestro version 10.4, schrodinger, NY; was used to prepare the crystal structure of human placental aromatase complexed with designed inhibitor HDDG046 (PDB ID: 4GL7). Most importantly, energy minimization was subjected to the imported target crystal structure to achieve a conformation, which harbors a low ΔG value which signifies the closeness of a molecule to the biological system. It implies the lowering of potential energy of the receptor and ligand under study. In addition, the water molecules were excluded from the proximity of 5Å of the ligand while the hydrogen atoms were added. The epik version 3.4 was used for modifying the protonation state of the imported crystal structure to the pH range of 7.0 ± 2.0. Apart from these, OPLS 2005 force field was utilized for performing geometrical modifications to a maximum root mean square deviation (RMSD) of 0.3Å [36-38].

Ligand Preparation

These molecules were exposed to the process of minimization of energy. It was carried out by the OPLS force field in a manner that the energy disparity among the designed molecules vestiges 0.001 kJ/mol Å. Furthermore, LigPrep version 3.0, Schrodinger, LLC, New York, NY was investigated for different potential tautomer of designed molecules such that

their spatial arrangement of atoms is intact. Similarly, like enzyme preparation, the ionization states were incorporated to the molecules with the help of epik version 3.4. Finally, on the basis of torsional angles, a particular ligand was selected.

Molecular Modeling Study

The molecular modeling predictions were estimated using glide platform. Docking refers to the assessment of the binding affinity between the newly designed molecules of flavonoids from LigPrep 3.0 and the selected target of human placental aromatase enzyme which was subjected to enzyme preparation. The potential binding active sites were recognized using glide program. Most importantly, glide uses its accurate binding prediction mode to attain results with lower RMSD from the native co-crystallized structures. In this regard, a grid setup was built for performing molecular modeling studies with the grid box configuration as 30×30×30 Å and 10×10×10 Å for inner box. The van der waals radii scaling of 0.7 for the proteins was performed to sustain the maximum number of 16 poses per ligand and the residues within the proximity of 5.0 Å of ligand poses were kept free to move in the prime refinement step. Ultimately, a designed molecule of low energy with appropriate chirality was subjected to molecular modeling predictions with a setup of "Extra Precision mode (Glide XP)". The experiential scoring function has been enhanced by the addition of the water desolvation terms and specific molecular recognition patterns. Of all the collective results, the molecule with a position harboring the least delta G value during the interaction with the enzyme is selected and analyzed[39].

ADMET Predictions

To assure the clearance of the newly designed drug in the clinical phase, ADMET (Absorption, Distribution, Metabolism, Excretion and Toxicity) predictions are essential. So, the drugs of optimum required characteristics can be screened while those with the undesired properties can be ruled out[40]. In this study, we have used the QikProp platform (version 4.6, 2015) and pkCSM which include the features of lead generation, lead optimization, improving accuracy and predicting ADMET for the ligand under observation. Kerns E.H *et al.* has exhibited a linkage between *in vivo* pharmacological activity and *in vitro* assay[41]. Moreover, the Veber rule suggests that if the number of rotatable bonds are not more than 10 then it represents good oral bioavailability. Apart from this, Abraham *et al.* stated that the Log P values are affected by the parameters like molecular volume, dipolarity, H- bond acidity and H- bond alkalinity[42]. Additionally, toxicity methods include hERG block assays, mutagenicity/ genotoxicity, micronucleus essay, Comet assay, Ames assay, MTT human hepatotoxicity assay and many more can be performed using QikProp.

Here, a myriad of drug associated characteristics of designed molecules of flavonoids were assessed using QikProp platform which are substantial for screening and characterizing as lead compounds. The parameters which are examined are as follows: H-bond Donor (0.0-6.0), H-bond Acceptor (2.0-20.0), Predicted water/gas partition coefficient (QPlogpw) (5.0-48.0), Predicted octanol/water partition coefficient (QPlogPo/w) (-2.0 to 6.5), Predicted aqueous solubility (QPlogS) (-6.0 to 0.5). Here, the bracketed scores represent the standard marks for respective properties[43]. Additionally, in this present study we have subjected our lead molecule forcomprehensive ADMET predictions using pkCSM platform which is based on graph-based signatures mainly using machine learning approaches. This platform aids in predicting certain critical parameters such as Caco2 permeability, BBB permeability, interaction of ligand with P- glycoprotein and CYP enzymes, total clearance, AMES toxicity, maximum tolerated dose for humans, hERG I and II interaction, oral rat toxicity studies, skin sensitization, minnow toxicity and many more[36].

Results and Discussions

The results of all the designed structures (2A-2X, 4A-4X, 6A-6X, 8A-8X and 10A-10X) docked with the target human placental aromatase were compared to the docking results of HDDG046 compound with the same target. Moreover, Table I to Table V reveal the binding energy, electrostatic energy, hydrogen bonding and hydrophobic interaction for all the series of compound designed. Most importantly, Figure 6 demonstrates the H-bonding interaction formed between the MET 374 of target and the ketone group of the pentagon ring. Additionally, other active sites for PDB: 4GL7 is investigated to be ARG 115, LEU 477, LEU 372, PHE 221, HIE 480, ARG 192, SER 478, VAL 313, VAL 369, THR 310, VAL 370, TRP 224, ALA 306, ASH 309, ILE 305, ILE 133, PHE 134 and VAL 373.

Molecular Modeling study of compounds (2A-2X)

2A-2X compounds were subjected to molecular modeling predictions which ultimately revealed a range

Table I — Molecular Modeling prediction for compound 2A-2X

Title	Docking score	Glide emodel	XP Hbond	XP PhobEn	XP Electro
2A	−5.943	−45.268	−0.7	−0.245	−0.11
2B	−6.755	−47.767	−0.462	−1.151	−0.344
2C	−4.688	−50.401	−0.35	0	−0.072
2D	−4.206	−39.297	−0.7	−0.442	−0.172
2E	−5.616	−35.181	0	−1.162	0.076
2F	−6.343	−41.562	0	−1.341	−0.082
2G	−5.416	−40.712	0	−0.745	−0.019
2H	−7.312	−41.163	−0.688	−0.54	−0.194
2I	−6.794	−36.697	−0.24	−0.807	−0.188
2J	−5.783	−36.289	−0.289	−0.912	−0.229
2K	−8.31	−46.395	−0.69	−1.08	−0.362
2L	−6.675	−41.737	0	−0.826	−0.064
2M	−3.784	−43.484	0	−0.286	−0.196
2N	−5.132	−36.967	−0.193	−0.55	−0.1
2O	−5.758	−45.138	−0.7	−0.125	−0.12
2P	−4.521	−44.187	−0.643	−0.519	−0.348
2Q	−4.383	−40.553	−0.7	−0.5	−0.211
2R	−6.063	−37.332	0	−1.396	−0.116
2S	−6.431	−42.191	0	−1.218	−0.039
2T	−6.991	−52.549	−1.625	−0.284	−0.627
2U	−8.204	−47.83	−1.845	−1.254	−0.637
2V	−6.882	−48.36	−0.7	−0.211	−0.434
2W	−6.25	−40.016	−0.406	−1.612	−0.154
2X	−5.349	−36.181	0	−1.071	0.061
HDDG046	−8.611	−69.782	−0.7	−0.95	−0.213

Table II — Molecular Modeling prediction for compound 4A-4X

Title	Docking score	Glide emodel	XP Hbond	XP PhobEn	XP Electro
4A	−5.469	−48.02	−0.7	−0.575	−0.137
4B	−7.294	−49.911	−1.277	−0.593	−0.415
4C	−5.791	−42.768	−1.246	−0.35	−0.385
4D	−5.752	−45.561	−0.659	−0.625	−0.119
4E	−5.603	−41.271	−0.394	−0.55	−0.166
4F	−5.757	−48.063	−0.393	−1.021	−0.208
4G	−4.34	−41.889	−0.526	−0.479	−0.219
4H	−7.317	−45.446	−0.582	−0.477	−0.178
4I	−6.359	−37.38	−0.564	−1.107	−0.147
4J	−6.667	−48.163	−0.49	−0.426	−0.315
4K	−8.679	−48.067	−0.616	−1.019	−0.337
4L	−5.304	−51.878	−0.485	−0.879	−0.352
4M	−6.98	−47.02	0	−0.51	−0.057
4N	−5.53	−43.558	0	−0.519	−0.076
4O	−6.038	−52.805	−0.699	−0.4	−0.126
4P	−5.334	−44.715	0	−0.361	0.008
4Q	−5.779	−49.211	−0.7	−0.634	−0.135
4R	−5.252	−40.735	−0.7	−0.589	−0.164
4S	−6.06	−46.907	−0.7	−0.75	−0.235
4T	−8.27	−52.09	−1.905	−1.194	−0.671
4U	−8.27	−52.09	−1.905	−1.194	−0.671
4V	−4.895	−44.701	−0.18	−0.943	−0.196
4W	−5.863	−40.415	−0.358	−1.125	−0.157
4X	−5.59	−43.698	0	−0.519	−0.076
HDDG046	−8.611	−69.782	−0.7	−0.95	−0.213

Table III — Molecular Modeling prediction for compound 6A-6X

Title	Docking score	Glide emodel	XP Hbond	XP PhobEn	XP Electro
6A	−6.9	−57.726	−0.683	−0.81	−0.167
6B	−7.088	−59.347	−0.7	−0.919	−0.385
6C	−6.605	−54.988	−0.7	−1.14	−0.208
6D	−7.027	−59.201	0	−0.841	−0.011
6E	−6.578	−54.845	0	−0.7	−0.118
6F	−7.292	−58.804	0	−0.9	0.034
6G	−7.087	−53.528	−0.591	−1.04	−0.164
6H	−6.01	−43.791	0	−1.051	−0.136
6I	−6.339	−46.37	0	−0.939	−0.027
6J	−6.897	−49.476	−0.417	−0.569	−0.209
6K	−8.169	−45.196	−0.673	−0.9	−0.338
6L	−7.59	−53.035	0	−1.162	−0.077
6M	−6.086	−47.3	0	−0.95	0.208
6N	−6.44	−55.048	−0.106	−1.407	−0.085
6O	−7.202	−62.96	0	−1.206	−0.147
6P	−6.77	−51.865	−0.7	−0.601	−0.124
6Q	−7.268	−60.422	0	−0.94	−0.012
6R	−6.446	−45.869	0	−0.899	0.007
6S	−6.974	−60.874	0	−0.832	0.044
6T	−7.033	−62.902	−1.625	−0.327	−0.645
6U	−8.005	−63.165	−0.96	−0.675	−0.112
6V	−7.129	−45.965	−0.688	−0.87	−0.336
6W	−6.565	−46.889	−0.7	−0.24	−0.332
6X	−6.755	−51.053	0	−1.225	−0.066
HDDG046	−8.611	−69.782	−0.7	−0.95	−0.213

Table IV — Molecular Modeling prediction for compound 8A-8X

Title	Docking score	Glide emodel	XP Hbond	XP PhobEn	XP Electro
8A	−7.088	−59.347	−0.7	−0.919	−0.385
8B	−7.569	−52.731	−0.67	−0.664	−0.259
8C	−6.605	−54.988	−0.7	−1.14	−0.208
8D	−6.622	−54.083	0	−0.837	−0.187
8E	−6.802	−49.425	0	−0.85	−0.174
8F	−7.044	−48.033	0	−0.902	−0.095
8G	−5.93	−50.213	−0.35	−0.868	−0.06
8H	−6.002	−44.411	0	−0.472	−0.118
8I	−6.449	−39.164	0	−0.678	0.054
8J	−6.448	−48.444	−0.3	−0.637	−0.176
8K	−6.597	−49.399	0	−0.818	−0.15
8L	−7.158	−47.651	0	−1.381	−0.156
8M	−3.784	−43.484	0	−0.286	−0.196
8N	−6.2	−52.018	0	−0.427	−0.015
8O	−5.758	−45.138	−0.7	−0.125	−0.12
8P	−6.77	−51.865	−0.7	−0.601	−0.124
8Q	−6.886	−58.978	0	−0.925	−0.204
8R	−6.97	−45.754	0	−0.814	−0.135
8S	−6.431	−48.575	0	−0.964	−0.095
8T	−7.555	−65.246	−1.2	−0.206	−0.612
8U	−7.743	−62.716	−1.92	−0.341	−0.639
8V	−6.557	−51.801	0	−1.057	−0.319
8W	−9.035	−47.008	−1.103	−1.45	−0.611
8X	−5.701	−42.314	0	−0.789	0.041
HDDG046	−8.611	−69.782	−0.7	−0.95	−0.213

Table V — Molecular Modeling prediction for compound 10A-10X

Title	Docking score	Glide emodel	XP Hbond	XP PhobEn	XP Electro
10A	−6.233	−51.369	−1.33	−0.614	−0.338
10B	−7.001	−45.079	−1.117	−0.819	−0.438
10C	−5.253	−44.354	−0.394	−0.652	−0.345
10D	−6.774	−47.317	−0.7	−0.739	−0.377
10E	−6.619	−44.126	−0.7	−0.815	−0.347
10F	−5.95	−44.858	−0.622	−1.077	−0.265
10G	−6.845	−45.103	−0.663	−1.026	−0.267
10H	−6.144	−46.083	−0.7	−1.016	−0.432
10I	−6.434	−46.688	−0.7	−0.883	−0.411
10J	−6.305	−41.685	−0.7	−0.894	−0.167
10K	−8.184	−47.763	−0.7	−0.985	−0.45
10L	−6.024	−50.715	−1.339	−0.326	−0.693
10M	−5.704	−54.33	−0.465	0	−0.265
10N	−5.97	−46.742	−0.7	0	−0.341
10O	−6.026	−53.874	−1.162	−0.591	−0.311
10P	−6.737	−47.026	−0.7	−0.748	−0.38
10Q	−6.955	−46.717	−0.7	−0.743	−0.381
10R	−6.58	−42.475	−0.543	−1.092	−0.287
10S	−6.013	−46.478	−0.647	−1.113	−0.267
10T	−7.436	−55.669	−1.964	−0.242	−0.67
10U	−7.34	−49.269	−2.086	−0.534	−0.433
10V	−5.991	−43.617	−0.7	−1.121	−0.571
10W	−5.654	−44.394	−0.212	−0.979	−0.41
10X	−6.143	−47.47	−0.603	−0.771	−0.269
HDDG046	−8.611	−69.782	−0.7	−0.95	−0.213

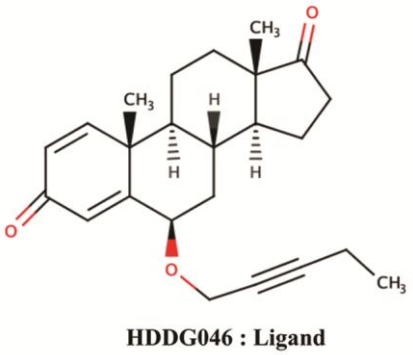

HDDG046 : Ligand

Figure 6 — Molecular modeling prediction for compound HDDG046

of docking score from -8.31 to -4.206 kcal/mol (Table I), where the lowest being the -8.31kcal/mol for compound 2K. This score is considered to be of substantial importance. Moreover, the docking score for HDDG046 (10,13-dimethyl-6-(pent-2-yn-1-yloxy)-7, 8, 9, 10, 11, 12, 13, 14, 15, 16-decahydro-3H-cyclopenta phenanthrene-3,17(6H)-dione) was found to be -8.611kcal/mol which is comparable to our designed molecule **2K**. Apart from this, the Figure 7 showcases H- bonding between the "**N**" of pyridine ring of **2K** and MET 374 of our target. In addition, the π – π stacking of the pyridine ring is associated with ARG 115.

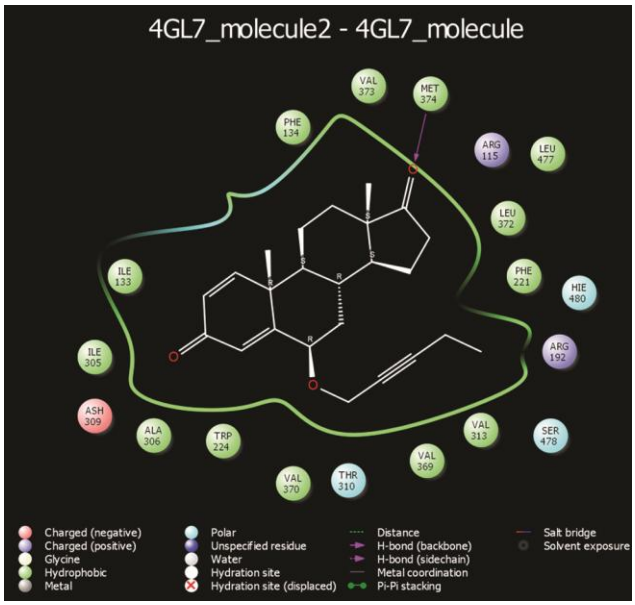

Figure 7 — Molecular modeling prediction for compound 2K

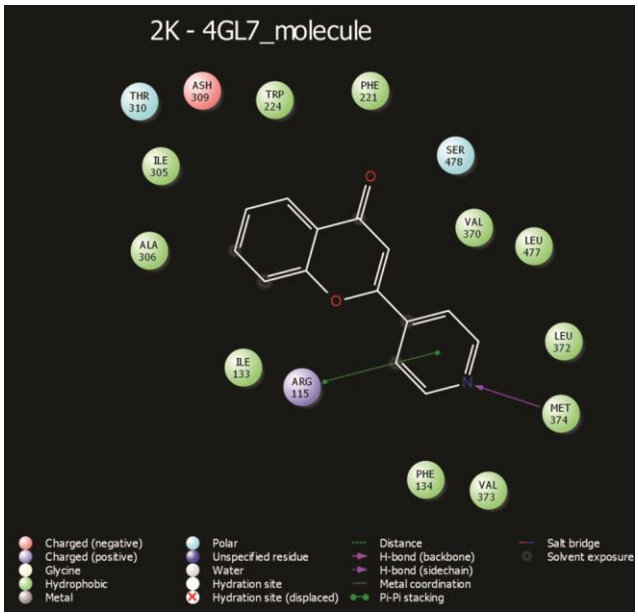

Figure 8 — Molecular modeling prediction for compound 4K

Molecular Modeling study of compounds (4A-4X)

The compounds **4A-4X** demonstrated a range of docking score -8.679 to -4.34 kcal/mol (Table II) with the target under study. Moreover, the lowest score was exhibited by compound **4K**. In this regard, the Figure 8 validated the H- bonding between the **"N"** of pyridine ring of **4K** and MET 374 of the target. Also, the ARG 115 and pyridine ring were found to have π – π stacking. In this case also, the docking score for 4K is of significant importance when compared to the HDDG046 ligand under comparison study.

Molecular Modeling study of compounds (6A-6X)

Juxtaposing the docking results of **6A-6X** compounds exhibited a low range score of -8.005 to -6.01kcal/mol (Table III) for all the compounds except **6K**, which has the binding energy as -8.169 kcal/mol. It was also found to have similar interaction with the target enzyme i.e. the **"N"** of pyridine ring forms hydrogen bond with MET374 and the pyridine's π system overlaps with ARG115. To corroborate, π – π stacking was observed in this case also (Figure 9).

Molecular Modeling study of compounds (8A-8X)

The compound series of **8A-8X** is found to have comparatively notable docking scores than the other series in this incumbent study. Most importantly, the range of docking score witnessed in this series is from -9.035 to -3.784 kcal/mol (Table IV). **8W** molecule showed the binding energy as -9.035 kcal/mol, which is the lowest of all the designed compounds including the ligand HDDG046. The –NH group of imidazole ring in **8W** molecule is predicted to have H-bonding interaction with ASH309. In addition, the π – π stacking is observed with the imidazole ring and PHE221. As a result of which it establishes credibility to be a prospective aromatase inhibitor on the basis of docking reports (Figure 10).

Molecular modeling study of compounds (10A-10X)

The compounds **10K** and **10L** from the series **10A-10X** has docking score -8.184and -5.253kcal/mol where the least value attributed to compound **10K** which is comparable to the docking score of HDDG046 (Table V). Moreover, the molecule **10K** forms the H-bonding interaction by using **"N"** of pyridine ring and MET 374. Additionally, the π – π stacking in **10K** is noted to be with ARG 115. So, it can be considered as potential aromatase inhibitors based on the molecular modeling predictions (Figure 11).

ADMET Predictions using QuikProp and pkCSM

Initially, the best selected molecules from each of the series were subjected to QuikProp and a single

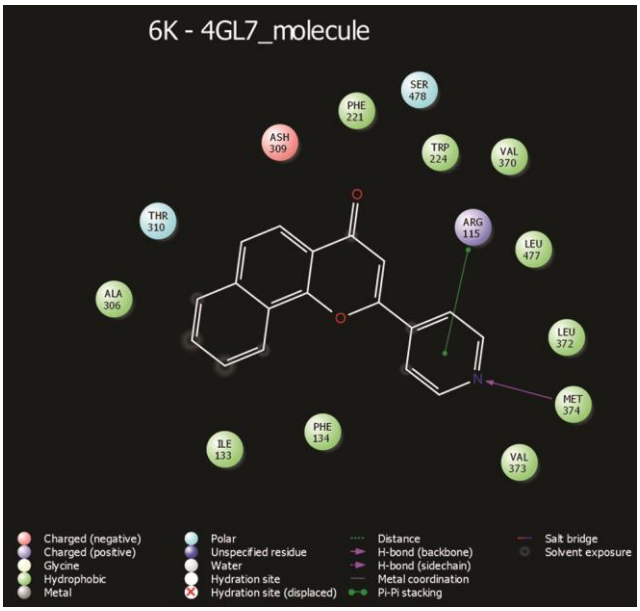

Figure 10 — Molecular modeling prediction for compound 8W

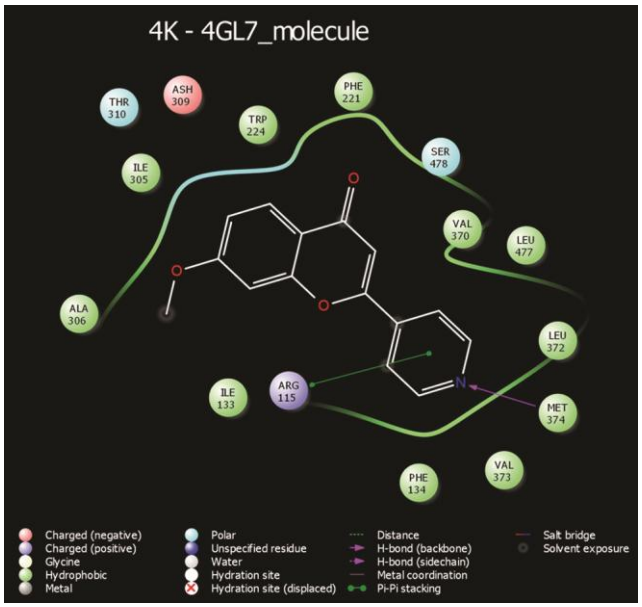

Figure 9 — Molecular modeling prediction for compound 6K

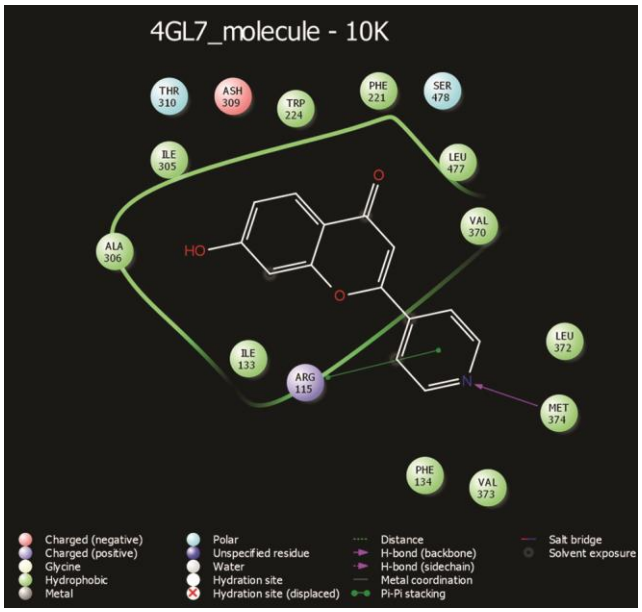

Figure 11 — Molecular modeling prediction for compound 10K

molecule was selected from the results which was further applied to pkCSM for a detailed ADMET study (Table VI).

The newly designed molecule 8W exhibits significant potential among the parameters such as QlogPoct, QPlogPw, QPlogPo/w and QPlogS of QuickProp.Its implication is comparable with HDDG046 and subsequently, both 8W and HDDG046 were studied using pkCSM.

Here, the Caco2 permeability is considered as higher if its value is greater than 0.90(log Papp in 10^{-6} cm/s). In this regard; as per Table VII, Caco2 permeability of 8W is estimated to be slightly higher than HDDG046. Moreover, the intestinal absorption is found to be prime for both the molecules as it is quite higher than the poorly absorbed drugs (>30%; normal range for optimally absorbed drugs). However, the skin permeability of HDDG046 (-3.197) is found to be lesser than 8W (-2.735). The drugs with logKp > -2.5 are considered to cross the skin barriers in dearth. CNS permeability for 8W is deduced to be optimum (greater than -2) while that of HDDG046 is comparatively reduced. To a fortiori, 8W is noted to be a substrate for P- glycoprotein, which is useful for the distribution of drug locally; ultimately modifying the metabolism and

Table VI — ADME study of compounds 2K, 4K, 6K, 8W, 10K and HDDG046 conducted by QuickProp

Sr. No.	Compound ID	QPlog Poct	QPlog Pw	QPlog Po/w	QPlog S
		(8.0-43.0)*	(5.0-48.0)*	(−2.0-6.0)*	(−0.6-0.5)*
1	2K	11.158	7.777	2.023	−2.648
2	4K	11.999	7.985	2.062	−2.681
3	6K	13.377	8.351	2.957	−3.779
4	8W	14.871	10.153	2.318	−3.709
5	10K	13.177	9.87	1.515	−2.901
6	HDDG046	16.776	7.52	3.919	−5.629

Table VII — Comprehensive ADMET predictions of HDDG046 and 8W using pkCSM

Property	Model Name	Predicted Value (HDDG046)	Predicted Value (8W)	Unit
Absorption	Water solubility	−5.117	−2.886	Numeric (log mol/L)
	$CaCo_2$ permeability	1.226	1.235	Numeric (log Papp in 10^{-6} cm/s)
	Intestinal absorption (human)	99.238	91.826	Numeric (% Absorbed)
	Skin Permeability	−3.197	−2.735	Numeric (log Kp)
	P-glycoprotein substrate	No	Yes	Categorical (Yes/No)
	P-glycoprotein I inhibitor	Yes	Yes	Categorical (Yes/No)
	P-glycoprotein II inhibitor	Yes	Yes	Categorical (Yes/No)
Distribution	VDss (human)	0.302	0.076	Numeric (log L/kg)
	Fraction unbound (human)	0.042	0.128	Numeric (Fu)
	BBB permeability	−0.039	0.593	Numeric (log BB)
	CNS permeability	−2.44	−1.831	Numeric (log PS)
Metabolism	CYP2D6 substrate	No	No	Categorical (Yes/No)
	CYP3A4 substrate	Yes	Yes	Categorical (Yes/No)
	CYP1A2 inhibitior	No	Yes	Categorical (Yes/No)
	CYP2C19 inhibitior	No	Yes	Categorical (Yes/No)
	CYP2C9 inhibitior	No	No	Categorical (Yes/No)
	CYP2D6 inhibitior	No	Yes	Categorical (Yes/No)
	CYP3A4 inhibitior	No	Yes	Categorical (Yes/No)
Excretion	Total Clearance	0.698	0.715	Numeric (log ml/min/kg)
	Renal OCT2 substrate	Yes	Yes	Categorical (Yes/No)
Toxicity Toxicity	AMES toxicity	No	Yes	Categorical (Yes/No)
	Max. tolerated dose (human)	−0.357	0.278	Numeric (log mg/kg/day)
	hERG I inhibitor	No	No	Categorical (Yes/No)
	hERG II inhibitor	Yes	Yes	Categorical (Yes/No)
	Oral Rat Acute Toxicity (LD50)	1.364	2.489	Numeric (mol/kg)
	Oral Rat Chronic Toxicity (LOAEL)	1.535	−0.1	Numeric (log mg/kg_bw/day)
	Hepatotoxicity	No	No	Categorical (Yes/No)
	Skin Sensitization	No	No	Categorical (Yes/No)
	T.Pyriformis toxicity	0.875	0.285	Numeric (log ug/L)
	Minnow toxicity	0.462	1.781	Numeric (log mM)

excretion properties. Apart from this, the oral rat acute toxicity i.e the LD_{50} value for 8W is found to be 2.489 mol/kg, which is quite higher than 1.364 mol/kg for HDDG046. This implies that the therapeutic window for our designed molecule 8W will be considerably bigger than that of reported compound HDDG046.

Conclusion

In this incumbent study of predicting novel flavonoid derivatives for inhibiting human placental aromatase in view to treat breast cancer, several molecules like **2K, 4K, 6K, 8W** and **10K** revealed noteworthy importance. Out of which, the molecule **8W** is found to be a potential inhibitor based on its molecular modeling studies and ADMET predictions. The docking score for **8W** is estimated to be -9.035 kcal/mol which is substantially better than the score of HDDG046 i.e. -8.611 kcal/mol. This molecule was considered to be superior among the series based on the docking results and mainly through the broad study by pkCSM platform. With relevance to solubility, permeability, enzyme/transporter interactions and toxicity studies, 8W molecule has corroborated its veracity to become a lead molecule in near future, as it tends to have optimum criteria to suffice the lead discovery process in coming years.

Conflict of Interest

Authors have no conflict of interest.

Acknowledgement

The authors thank the Gujarat Council of Science and Technology (GUJCOST, Gandhinagar, Gujarat, India) for financial assistance (under Minor Research Project) and also thankful to Raghu Rangaswamy, Anirban Banerjee and Vinod Devaraji (Schrödinger team) for providing licensed version of Maestro 10.4, Schrödinger. The authors also acknowledge Ramanbhai Patel College of Pharmacy, Charotar University of Science and Technology, Changa (CHARUSAT) for providing the necessary infrastructure to carry out the research.

References

1 Yue W, *Int J Cancer*, 127(8) (2010) 1748.
2 Russo J & Russo I H, *J Ster Biochem and Mol Biol*, 102 (2006) 89.
3 Russo I H & Russo J, *Envir Health Persp*, 104(9) (1996) 938.
4 Viciano I, Marti S, *J Phy Chem B*, 120(13) (2016) 333.
5 Van Meeuwen J A, Ter Burg W, Piersma A H, Van Den Berg M & Sanderson J T, *Food and Chem Tox*, 45(11) (2007) 2319.
6 Vaz A D, Cytochrome Activation by Cytochromes P450: A Role for Multiple Oxidants in the Oxidation of Substrates.
7 Ghosh D, *J Med Chem*, 55(19) (2012) 8464.
8 Fabian C J, *Int J Clin Pra*, 61(12) (2007) 2051.
9 Sporn M B & Lippman S M, 'Agents for chemoprevention and their mechanism of action', in *Holland-Frei Cancer Medicine*, 6th edn (BC Decker, Hamilton) (2003).
10 Dutertre M, Smith CL, Molecular mechanisms of selective estrogen receptor modulator (SERM) action. *J of Pharmacology and Exp Ther*, 295(2) (2000) 431.
11 Balunas MJ, Brueggemeier RW, Kinghorn AD, *Anti-Can Agents in Med Chem*, (6) (2008) 646.
12 Lorizio W et.al, *Breast Can Res and Treat*, 132(3) (2012) 1107.
13 Nielsen AJ, McNulty J, *Med Res Rev*, 39(4) (2019) 1274.
14 Schneider Y et.al, *Int J of Cancer*, 107(2) (2003) 189.
15 Rimando AM et. al, *J of Agri and Food Chem*, 50(12) (2002) 3453.
16 Nakagawa H et. al, *J of Can Res and Clin Onclogy*, 127(4) (2001) 258.
17 Abdel Bar FM, Abbas GM, Gohar AA, Lahloub MF, *Nat Prod Res*, (2019) 1.
18 Chung EY et. al, *Planta medica*, 69(08) (2003) 710.
19 Kumar S, Pandey AK, *The Sci World J*, (2013) 1.
20 Panche AN, Diwan AD, Chandra SR, *J of Nut Sci*, 5(e47) (2016) 1.
21 Narayana KR, Reddy MS, Chaluvadi MR, Krisha DR, *Ind J of Pharmacology*, 33(1) (2001) 2.
22 Lephart ED, *Enz Res*, Volume (2015) 1.
23 Kao YC, Environental Health Perspectives, 106(2) (1998) 85.
24 Shah U, Patel S, Patel M, Gandhi K, Patel A, *Indian Journal of Chemistry – B*, 59B (2020) 283.
25 Pouget, C et.al, *Pharm Res*, 19(3) (2002) 286.
26 Sanderson JT, Boerma J, Lansbergen GW, van den Berg M, *Tox and App Pharmacology*, *182*(1) (2002) 44.
27 Yahiaoui S et.al, *Bio & Med Chem Let*, 14(20) (2004) 5215.
28 Pouget C, Lauthier F, Simon A, Fagnere C, *Bioorg & Med Chem Lett*, 11(24) (2001) 3095.
29 Ibrahim AR, Yusuf J, Haji A, *The J of Ster Biochem and Mol Bio*, 37(02) (1990) 257.
30 Yahiaoui S et.al, *Eur J of Med Chem*, 46(06) (2012) 2541.
31 Yahiaoui S et.al, *Bioorg & Med Chem Lett*, 16(3) (2008) 1474.
32 Patel S, Shah U, *Asian J of Pharm and Clin Res*, 10(02) (2017) 403.
33 de Ruyck J, Brysbaert G, Blossey R, Lensink MF, *Adv and App in Bioinf and Chem*, 9 (2016) 1.
34 Pettersen EF et. al, *J of Comp Chem*, *25*(13) (2004) 1605.
35 Grosdidier A, Zoete V, Michielin O, *Nucleic Acids Research*, *39*(2) (2011) W270.
36 Shah U, Patel S, Patel M, Upadhayay J, *Let in Drug Des & Dis*, *14*(11) (2017) 1267.
37 Schrodinger Tutorial. Msi.umn.edu/sites/default/files/SchrodingerTutorial2011.html (Assessed on November 28, 2019)
38 Glide user manual. Isp.ncifcrf.gov/files/isp/uploads/2010/07/gli55_user_manual.html (Assessed on November 28, 2019)
39 Ikram N et.al, *Biomolecules*, 9(4) (2019) 1.
40 QikProp [Internet]. QikProp | Schrödinger. [cited 2019Nov28]. Available from: https://www.schrodinger.com/qikprop
41 Kerns, Edward & Di, Li. (2008). Drug-Like Properties: Concept, Structure Design and Methods, From ADME to Toxicity Optimization.
42 Abraham MH, Chadha HS, Leitao RA, Mitchell RC, Lambert WJ, Kaliszan R, Nasal A, Haber P. *Journal of Chromatography A*. 766(1-2) (1998) 35.
43 Pires DE, Blundell TL, Ascher DB, *J Med Chem*, 58(9) (2015) 4066.